

DMD #12328

TITLE:

The Disposition and Metabolism of Naveglitazar, a Peroxisome Proliferator-activated Receptor (PPAR)
 α - γ dual, γ -dominant agonist in Mice, Rats, and Monkeys.

AUTHORS:

Ping Yi, Chad E. Hadden, William F. Annes, David A. Jackson, Barry C. Peterson, Todd A. Gillespie,
and Jason T. Johnson*

*Corresponding author.

LABORATORY ADDRESS:

Lilly Research Laboratories, Department of Drug Disposition, Eli Lilly and Company, Lilly Corporate
Center, Indianapolis, IN 46285, USA.

DMD #12328

RUNNING TITLE:

Disposition and Metabolism of Naveglitazar in Animals.

Corresponding author: Jason T. Johnson, Lilly Research Laboratories, Department of Drug Disposition, Eli Lilly and Company, Lilly Corporate Center, Indianapolis, IN 46285, USA. Telephone: (317) 276-9251; Fax: (317) 433-6432; E-mail: johnson_jason_t@lilly.com

Number of text pages: 37

Number of Tables: 6

Number of Figures: 9

Number of References: 17

Number of words in Abstract: 249

Number of words in Introduction: 356

Number of words in Discussion: 968

Non-standard abbreviations:

HPLC (High Performance Liquid Chromatography), LC/MS and LC-MS/MS (liquid chromatography with tandem mass spectrometric detection), LSC (liquid scintillation counting), AUC (area under the plasma concentration versus time curve), C_{\max} (maximum plasma concentration), T_{\max} (time to reach maximum plasma concentration), k_e (elimination rate constant), $t_{1/2}$ (half-life), MRT (mean residence time), AUMC (total area under the first moment of the drug concentration curve), V_{ss} (volume of distribution at steady state), V_{ss}/F (apparent volume of distribution at steady state).

DMD #12328

ABSTRACT:

Naveglitazar (LY519818) is a non-thiozolidinedione peroxisome proliferator-activated receptor (PPAR) α - γ dual, γ -dominant agonist that has shown glucose lowering potential in animal models and in the clinic. Studies have been conducted to characterize the disposition, metabolism, and excretion of naveglitazar in mice, rats, and monkeys after oral and/or intravenous (IV) bolus administration.

Following oral administration of [^{14}C]naveglitazar, naveglitazar was well absorbed and moderately metabolized in all species evaluated with total recoveries of radioactivity ranging from 90 to 96%.

Naveglitazar was the most abundant peak observed in circulation at C_{max} representing 68 to 81% of the total radioactivity in plasma. The most prominent metabolite observed in circulation was the *R*-enantiomer of naveglitazar, LY591026, which is formed via enzymatic chiral inversion. *Para*-hydroxy naveglitazar and the sulfate conjugate of *para*-hydroxy naveglitazar were also observed in circulation in most species, especially in the monkey. The metabolic pathways observed include enzymatic chiral inversion, aromatic hydroxylation, oxidative dehydrogenation, and/or various phase II conjugation pathways. Naveglitazar was highly bound to plasma proteins among the species examined (> 99%) and binding was independent of concentration. Biliary excretion was recognized as the most prominent excretion pathway in bile-duct cannulated rats (79 out of the 96% recovered), producing an acyl glucuronide conjugate of naveglitazar and a sulfate and glucuronide diconjugate of *para*-hydroxy naveglitazar which were shown to be reversible. The primary excretory pathway observed in mice and monkeys was via the feces. In summary, naveglitazar was well absorbed, moderately metabolized, and excreted via the feces in mice, rats, and monkeys.

DMD #12328

Type 2 diabetes mellitus is a major and expanding health issue throughout the world (Burke et al., 1999). This form of diabetes, which includes approximately 90% of all such cases, is characterized by hepatic and peripheral insulin resistance and impaired β -cell function and insulin secretion (Diamant and Heine, 2003). In addition to elevated glucose levels, type 2 diabetes is most often associated with a variety of cardiovascular risk factors including dyslipidemia, hypertension, and obesity (DeFronzo, 1992; Ferrannini, 1998).

Naveglitazar (LY519818, benzenepropanoic acid, alpha-methoxy-4-[3-(4-phenoxyphenoxy)propoxy], (alpha S)-) (Figure 1), is a peroxisome proliferator-activated receptor (PPAR) α - γ dual, γ -dominant agonist. PPAR compounds are members of the nuclear receptor super family, and have been shown to play a role in lipid and carbohydrate homeostasis (Keller et al., 1993). PPAR γ , which is predominately expressed in adipose tissue, regulates the transcription of genes involved in glucose and lipid metabolism (Kersten et al., 2000; Auwerx, 1999). A class of agents known as thiazolidinediones (TZD) or glitazones, have been shown to modulate PPAR γ , resulting in lower plasma glucose, insulin, triglyceride, and fatty acid levels in humans with Type 2 diabetes (Olefsky, 2000; Schoonjans and Auwerx, 2000).

Naveglitazar, a non-TZD, functions as a potent and efficacious insulin sensitizer in rodents, possessing a novel profile that may be result in an improved therapeutic agent for the treatment of type 2 diabetes and associated dyslipidemia (Liu and Reifel-Miller, 2005). In type 2 diabetics, naveglitazar significantly reduced fasting serum glucose, fasting triglycerides and hemoglobin A1C, and significantly increased HDL cholesterol, displaying an efficacy comparable or superior to the currently marketed TZD rosiglitazone (Prince et al., 2004). As we continue to understand the functions of different subtypes of PPAR receptors and the complex metabolic disorders associated with type 2 diabetes, dual-PPAR agonist molecules may become a new class of therapeutic agents that may provide more favorable clinical outcomes for type 2 diabetics (Desvergne et al., 2004; Bond and Yates, 2004; Rizvi, 2004). The objective

DMD #12328

of this work was to characterize the disposition and metabolism of naveglitazar in mice, rats, and monkeys, which will aid in the safety assessment for this molecule as it relates to clinical practice.

DMD #12328

Materials and Methods

Materials. Naveglitazar (*S*-enantiomer, LY519818), [¹⁴C]naveglitazar (Figure 1), LY591026 (*R*-enantiomer), internal standard (Compound 487748), 4-hydroxy-naveglitazar (LY621631), O-sulfate of 4-hydroxy- naveglitazar sodium salt (LY2291229), and dehydrogenated naveglitazar (LY2419535) were synthesized at Eli Lilly and Company (Indianapolis, IN, USA). The radiochemical purity of [¹⁴C]naveglitazar was approximately 98% as determined by HPLC and the specific activity was 13.8 μCi/mg. [³H]naveglitazar Na (in a solution of 19272.7ng/mL) was obtained from Amersham Pharmacia Biotech (Piscataway, NJ). 4, 4'-dihydroxydiphenyl ether was obtained from TCI America (Portland, OR). 4-hydroxydiphenyl ether was obtained from Aldrich Chemical Company (Milwaukee, WI). The β-glucuronidase (type HP-2, from *Helix pomatia*) was purchased from Sigma Chemical Company (St Louis, MO). Ultima Flo M was purchased from PerkinElmer Life Sciences (Boston, MA). All other reagents and solvents were of analytical grade and were obtained commercially.

Animal Experiments. All animal experiments were conducted according to protocols approved by Eli Lilly Animal Care and Use Committee. All animals were acclimated to experimental conditions before use (at least 3 days for mice and rats, and at least 6 weeks for monkeys). Food and water were supplied ad libitum throughout the acclimation and experimental periods. The oral dose suspensions used in the studies were prepared with 1% carboxymethylcellulose sodium, 0.5% sodium lauryl sulfate, 0.085% povidone and 0.05% Dow Corning antiform1510 US in purified water. The dose solution used for intravenous administration in monkeys was prepared with 40% PEG300, 60% purified water, and 0.8% of 1N NaOH.

Dosing of Animals and Sample Collections. The single-dose plasma pharmacokinetics of naveglitazar, LY591026, and radioactivity were studied in male ICR mice, male Fischer 344 rats, and cynomolgus monkeys following oral administration of [¹⁴C]naveglitazar. A separate study was conducted in rats to evaluate the pharmacokinetics of naveglitazar and LY591026 following the administration of a single 10

DMD #12328

mg/kg dose of each compound. Mice and rats were administered a 10 mg/kg oral dose of [¹⁴C]naveglitazar with a specific activity of 50 μCi/kg. Monkeys were given a 1 mg/kg intravenous bolus (IV) or 5 mg/kg oral dose of [¹⁴C] naveglitazar with a specific activity of 10 μCi/kg.

Mice were divided into three groups. Group 1 animals (n = 3/time point) were housed in shoebox cages and were used to determine the pharmacokinetics of naveglitazar, LY591026, and radioactivity. Blood samples were collected for plasma from mice via cardiac puncture at 0.5, 1, 2, 4, 8, 12, 24, 48, 72, 96, and 120 hours post-dose. Group 2 mice were housed in metabolism cages (n = 3/cage) for the collection of excreta to determine the mass balance and metabolism of naveglitazar. Urine, feces, and cage wash were collected in 24 hour intervals for up to 120 hours. The third group of animals (n = 3/time point) were housed in shoebox cages and used to evaluate the metabolites present in plasma.

Rats were divided into three groups. Group 1 animals (n = 3/time point) were housed in shoebox cages and were used to determine the pharmacokinetics of naveglitazar, LY591026, and radioactivity. Blood samples were collected for plasma from rats via cardiac puncture at 0.5, 1, 2, 4, 8, 12, 24, 48, and 72 hours post-dose. Group 2 rats (n = 4) were individually housed in metabolism cages for the collection of excreta to determine the mass balance and metabolism of naveglitazar. Urine, feces, and cage wash were collected in 24 hour intervals for up to 120 hours. Group 3 animals, which were bile-cannulated rats (n = 4), were individually housed in metabolism cages for the collection of excreta to determine the mass balance and metabolism of naveglitazar. Urine, feces, and cage wash were collected in 24 hour intervals for up to 72 hours where as bile was collected in 8 hour intervals. In a separate study, rats were given naveglitazar or LY591026. In this study, blood samples for plasma were collected at 0.5, 1, 2, 4, 8, 12, and 24 hours to determine pharmacokinetics of each analyte.

Monkeys were divided into two groups. Group 1 animals (n = 4, 3 female and 1 male) received an oral dose and Group 2 (n = 4, 3 female and 1 male) received an intravenous (IV) dose of [¹⁴C] naveglitazar. All animals were housed in individual metabolism cages for collection of excreta. Blood samples were

DMD #12328

collected for plasma via the femoral vein at 0.083, 0.17, 0.25, 0.5, 1, 2, 4, 8, 12, 24, 48, 72, 96, 168, 240, 336, 408, 504, 576, and 672 hours post-dose following IV dosing and at 1, 2, 4, 8, 12, 24, 48, 72, 96, 168, 240, 336, 408, 504, 576, and 672 hours post-dose following oral dosing. Urine, feces, and cage wash were collected in 24 hour intervals for up to 672 hours post-dose. For all studies, blood was collected in tubes containing EDTA as the anticoagulant and plasma was obtained by centrifugation and stored at approximately -70°C until subsequent analysis.

Radioactivity Analysis. Radioactivity in plasma, urine, bile, and cage wash was determined by mixing aliquots of plasma, urine, bile, or cage wash (0.1 g) with approximately 12 mL of Beckman Ready Protein Plus or Packard Aquassure scintillation fluid (Packard Instruments, Meriden, CT) and counted in a liquid scintillation counter (Beckman LS5000TD, Beckman Instruments, Columbia, MD). Mouse and rat carcasses were gently boiled in a beaker containing ethanol and potassium hydroxide until all tissues were dissolved. Aliquots were mixed with scintillation fluid and acetic acid and then counted in a liquid scintillation counter. Radioactivity in fecal homogenates, which were prepared by soaking fecal samples in a 1:1 methanol/water (v, v) solution that was frozen, thawed, and then shaken vigorously, was measured by scintillation counting of trapped $^{14}\text{CO}_2$ after combustion of dried homogenate aliquots. Samples were combusted on a Packard Sample Oxidizer, Model 307 (Packard Instruments, Meriden, CT).

Plasma Protein Binding. Plasma protein binding of naveglitazar was investigated using a [^3H] naveglitazar and an ultracentrifugation technique. Mouse, rat, and monkey plasma was spiked at concentrations of 0.1, 1, 10, 100, and 1000 ng of [^3H] naveglitazar /mL and incubated for 1 hour at 37°C. After incubation, three 1.2 mL aliquots were centrifuged at 130,000 rpm for 3.25 hours at 37°C. Aliquots of the unbound fraction were diluted with 10 mL of scintillation fluid and analyzed by liquid scintillation counting (LSC).

In Vitro Incubations in Liver Slices. Liver slices from Fischer 344 rats, cynomolgus monkeys, and a human donor were prepared and incubated with a 50 μM concentration of naveglitazar (LY519818) for 4

DMD #12328

and 24 hours according to publishing procedures (Vandenbranden et al., 1998). After incubation, the slices were sonicated in their culture medium and the homogenates were extracted by protein precipitation with acetonitrile followed by centrifugation. The supernatants were used for metabolite analysis.

Metabolism Sample Preparation. Plasma and excreta samples from the single-dose pharmacokinetic and excretion studies were utilized to assess the metabolism of naveglitazar. Plasma samples were extracted by protein precipitation with acetonitrile. The extraction was conducted by adding acetonitrile (3 parts) to plasma (1 part, (v/v)). After the samples were mixed and centrifuged, the supernatants were transferred to silanized glass tubes, evaporated to dryness under nitrogen, and reconstituted with a 50/50 methanol/water solution. Urine samples were either directly injected (for those samples with high amounts of radioactivity) or extracted by solid phase extraction (SPE) using C18 or Waters Oasis MAX cartridges. For C18 SPE (ISI Isolute, 100 mg; Jones Chromatography, Lakewood, CO) extraction, the cartridge was conditioned with 1 mL of methanol followed by 1 mL of water. After conditioning, 1 mL of urine was loaded onto the cartridge followed by a washing step with 1 mL of water. The sample was then eluted with 1 mL of methanol, which was then concentrated to approximately 1/10 of the original volume by evaporation under nitrogen. For Waters Oasis MAX SPE (1cc; Waters Corporation, Milford, MA), the cartridge was conditioned with 1 mL of methanol followed by 1 mL of water. The urine sample was acidified with concentrated HCl (20 μ L of HCl was added to 1 mL of urine) and the acidified urine (1 mL) was loaded into the preconditioned cartridge. The cartridge was washed with 1 mL of 50 mM ammonium acetate/methanol (95/5). The sample was eluted with 1 mL of 2% formic acid in methanol. The eluted sample was evaporated to dryness under nitrogen and reconstituted in methanol/water (50/50). Bile samples were directly injected after centrifugation. Fecal samples were extracted with methanol. A 1 to 3 gram fecal homogenate was added to 2 to 6 mL of methanol, vortexed, mixed on a rotator for approximately 15 minutes, and then centrifuged. The supernatant was transferred to a silanized glass tube. The fecal extraction procedure was then repeated and the second supernatant was added to the first

DMD #12328

supernatant. The combined supernatant was then evaporated to dryness under nitrogen and reconstituted in methanol/water (50/50).

Metabolite Radioprofiling by HPLC. Metabolites in various matrices were separated on a reverse phase HPLC column with a Shimadzu LC-10 system. Mobile phase A consisted of 90% water, 5% methanol/acetonitrile (50:50), 5% isopropanol alcohol with 10 mM ammonium formate. Mobile phase B consisted of 5% water, 90% methanol/acetonitrile (50:50), 5% isopropanol alcohol with 10 mM ammonium formate. For plasma and fecal extracts from rats and monkeys, and urine from monkeys and mice, a Discovery C18 column (4.6mm x 150 mm, 5 μ m; Supelco, Bellefonte, PA) was used with the following gradient: 0 to 35 minutes, linear gradient from 0% to 75% B, 35 to 36 min, ramping to 90% B, 36 to 40 min, isocratic at 90% B, 40.0 to 40.1 min, ramping from 90% to 0% B. 40.1 to 50 min, isocratic at 0% B. The flow rate was 1 mL/min. To improve the separation of acyl glucuronide isomers, metabolites in rat bile were separated on a Keystone Fluophase RP column (2.1 mm x 150 mm, 5 μ m; Thermo Hypersil-Keystone Scientific Inc., Bellefonte, PA) with the gradient set as 0 to 3 min, isocratic at 10% B, 3 to 40 min, linear gradient to 50% B, 40.0 to 40.1, ramping to 90% B, 40.1 to 50 min, isocratic at 90% B, 50 to 50.1, ramping from 90% B to 10% B. 50.1 to 55 min, isocratic at 10% B. For mouse plasma and fecal extracts, a Luna C18 column (4.6 mm x 150 mm, 3 μ m; Phenomenex, Torrance, CA) was used to improve the separation of LY519818 and its taurine conjugate. The gradient was programmed as: 0 to 35 min, linear gradient from 20% to 75% B, 35 to 45 min, isocratic at 75% B, 45.0 to 45.1, ramping to 90% B, 45.1 to 50, isocratic at 90% B, 50.0 to 50.1, ramping from 90% B to 20% B, 50.1 to 57 min, isocratic at 20% B. The metabolites were detected by either a radiochemical detector (Berthold Z 5004, Bald Wildbad, Germany) equipped with a 500- μ L liquid cell (PerkinElmer Ultima Flo M) and scintillation fluid set at a flow rate of 3.5 mL/min or by HPLC fraction collection with subsequent radioactivity counting and chromatogram reconstruction. For fraction collection, HPLC effluent was collected into PerkinElmer 96-well LumaPlate at 15-second intervals. The plates were dried under

DMD #12328

centrifugal vacuum and counted on a Packard Microplate Scintillation & Luminescence counter (TopCount NXT, Packard Instrument Company, Downers Grove, IL). The radiochromatograms were reconstructed using the radioactivity (CPM or DPM) versus time data.

LC/MS and LC-MS/MS. LC/MS/MS analyses were conducted on a ion trap mass spectrometer (Finnigan LCQ Deca ThermoFinnigan, San Jose, CA) equipped with a Shimadzu LC-10 HPLC system. The mobile phases and gradients used in LC/MS analysis for all matrices were the same as those used for radioprofiling. Smaller diameters HPLC columns (2.1 mm X 150 mm) and slower flow rates (0.25 ml/min) were applied to improve the sensitivity of LC/MS analysis. Mass spectral analysis was performed with both positive and negative ion electrospray ionization. The capillary temperature was 225°C and the spray voltage was 5 kV. The full scan MS spectra were obtained from m/z 200 to m/z 1000. The MS/MS spectra were obtained with the collision energy set at 45%.

Hydrolysis of Conjugates. Glucuronide or sulfate conjugates in bile and plasma were hydrolyzed to their corresponding deconjugated metabolites by incubation with glucuronidase (containing both β -glucuronidase and sulfatase activities) in 0.2 M sodium acetate buffer, pH 5.0, at 37°C for up to 16 hours. The control incubations were conducted in the absence of glucuronidase.

NMR Sample Preparation and Analysis. Naveglitazar and the M7 metabolite (dehydrogenated parent) were separately dissolved in 150 μ L of deuteriochloroform and transferred to 3 mm NMR tubes. Data were acquired on a Varian INOVA 500 NMR spectrometer employed with a Varian gradient, triple-resonance IFC probe (LY-519818) or a Varian gradient, triple-resonance, Cold Probe. The suite of experiments included a standard proton, homonuclear GCOSY, direct-correlation multiplicity-edited HSQCAD, and long-range GHMBCAD. Data were referenced to the solvent at 7.27 ppm for ^1H and 77.2 ppm for ^{13}C . The air-dried sample of M7 was later dissolved in 150 μ L of deuteromethanol for the acquisition of a GBCPMG-HSQMBC for the measurement of long-range heteronuclear coupling constants.

DMD #12328

The M1 metabolite (sulfate conjugate of the para hydroxyl metabolite) was isolated from the rat liver slices incubated with naveglitazar for 24 hours. Column trapping was used to introduce the metabolite into the flow probe of the NMR. The metabolite was isolated and transferred to a 2mL HPLC injector loop connected to the LC/NMR. The LC was programmed to pump 2 mL/min of deuterium oxide. Using a flow splitter, 25% of this flow went through the loop and was then combined with the remainder of the flow in a 50 μ L static mixer. From the mixer, the flow was directed to a secondary trapping column (Thomson Liquid Chromatography, 30x3mm, TIC-PAQC 18, 5 μ m), where the metabolite was retained. The transfer of the analyte to the trapping column was monitored with the UV detector. When the transfer was complete (i.e. the UV absorbance returned to baseline) the flow was stopped, the mixer was removed and the trapping column was reoriented such that the flow through the column was reversed. The mobile phase was subsequently changed to 50% deuterium oxide and 50% deuterated acetonitrile in order to elute the metabolite from the secondary column and into the flow probe of the NMR. NMR data for M1 were acquired on a Varian INOVA 600 NMR spectrometer equipped with a triple-resonance flow probe. The suite of experiments included a standard proton with water elimination through transverse gradients, homonuclear WETDQCOSY and TOCSY, and through-space ROESY. Data were referenced to deuterated acetonitrile at 1.94 ppm for ^1H and 1.39 ppm for ^{13}C .

Chiral Assay for LY621631 (M2). M2 (*para*-hydroxy Naveglitazar), was isolated from mouse, rat, and monkey fecal extracts using a C18 HPLC column. The *S*- and *R*- enantiomers of this metabolite were separated via chiral chromatographic techniques using a chiral HPLC column (Keystone Chiral/beta-OH, 1mm x 250mm, 5 μ m). Mobile phase A consisting of 73:25:2/0.05 of acetonitrile:methanol:water:5 M ammonium formate and mobile phase B consisting of 60:38:2/0.05 of acetonitrile:methanol:water:5 M ammonium formate. The gradient was programmed as follows: 0 to 0.5 minutes, isocratic at 0% of B, 0.50 to 10 minutes, liner gradient from 0% to 20% of B, 10.0 to 10.1min, ramping to 100% B, 10.1 to 15.0 min, isocratic at 100% of B, 15.0 to 15.1 min, ramping from 100% to 0% of B. The run time was 25

DMD #12328

minutes. The flow rate was 250 $\mu\text{L}/\text{min}$. Peak detection was carried out by UV using a Surveyor PDA detector and by full scan MS and MS/MS using a Ion trap mass spectrometer (Finnigan LCQ Duo) in positive electrospray ionization mode with a spray voltage of 5 kV, capillary temperature at 225°C, and the collision energy at 45%.

Analytical Procedure. Naveglitazar and LY591026 in plasma were assayed using a validated 96-well solid-phase extraction (SPE) procedure with LC/MS/MS detection. Specifically, 10 μL of internal standard (2500 ng Compound 487748/mL) was added to sodium EDTA plasma (75, 100, or 200 μL for mouse, rat, or monkey, respectively) followed by the addition of 700 μL of 5:95 methanol:1% formic acid solution (v,v). A dry molecular sieve was added to each well of the collection block. The following steps on the procedure were performed on a Tomtec Quadra 96-well workstation (Model 320, Tomtec, Hamden, CT). Each well of the ANSYS C18 15 mg disk extraction block were conditioned with 250 μL of methanol followed by 300 μL of 5:95 methanol:formic acid (v,v). Each mixed sample was transferred to the SPE block and the samples were aspirated through the cartridge at an approximate flow rate of 200 $\mu\text{L}/\text{min}$. The cartridge bed was washed with 400 μL water followed by 250 μL of 23:75:0.1 methanol:water: 5 M ammonium formate (v,v,v). Full vacuum was applied for 30 seconds. A polypropylene collection block containing molecular sieves was placed into the vacuum manifold and the analytes were eluted from the cartridges with 150 μL acetonitrile at an approximate flow rate of 250 $\mu\text{L}/\text{min}$. The collection block was removed from the Tomtec Quadra workstation. The analyst then added 250 μL acetonitrile which was previously dried with molecular sieves to the collection block. A cover film was applied to the collection block and the samples were allowed to stand for a minimum of 2 hours. The collection block was then centrifuged at approximately 3000 rpm for 5 min. Extracts were transferred to a new block and then centrifuged at approximately 3000 rpm for 5 min. Extracts were placed in autosampler vials for analysis using selected reaction monitoring (SRM) turbo ion spray

DMD #12328

LC/MS/MS in the negative ion mode (naveglitazar and LY591026 $m/z = 421.1 \rightarrow 389.2$, LY487748 $m/z = 427.1 \rightarrow 395.1$). The LC/MS/MS instrument used was a SCIEX API-3000. The validation range of the assay for naveglitazar and LY591026 was approximately 1 to 5000 ng/mL in rat and monkey plasma and 2 to 5000 ng/mL in mouse plasma. The mean accuracy (relative error) for naveglitazar and LY591026 for all species evaluated was within 17% of the theoretical values across the entire standard curve range. The mean precision (%CV) for all species was $\leq 12\%$. Plasma samples exceeding the upper limit of quantitation were determined by dilution with control plasma.

Data Analysis. Plasma concentrations were calculated using the Applied Biosystems program MacQuan, version 1.6. Pharmacokinetic parameters were determined using standard noncompartmental methods via the proprietary ADME WINPTK computer software package (Eli Lilly and Company). AUC was calculated by the linear trapezoidal rule. Plasma clearance was calculated as the IV bolus dose divided by the plasma $AUC_{0-\infty}$. Values for C_{max} and T_{max} were obtained from observed data. The elimination rate constant, k_e , was determined by linear regression of the terminal log-linear phase of the concentration versus time curve. Terminal half-life ($t_{1/2}$) was calculated as $0.693/k_e$. The mean residence time (MRT) was calculated from the ratio of AUMC (total area under the first moment of the drug concentration curve) to AUC. The volume of distribution at steady state (V_{ss}) was calculated as clearance x MRT. The apparent volume of distribution (V_{ss}/F) was calculated as clearance/ k_e . Oral bioavailability in monkeys was estimated from the dose-adjusted ratio of the $AUC_{0-\infty}$ relative to that of the 5 mg/kg IV bolus dose. Samples below the limit of quantitation were assigned a value of zero for calculating kinetic parameters.

Percent protein binding of naveglitazar was calculated as follows: % Protein Binding = $(1 - C_f/C_p) \times 100$ where C_f = amount of radioactivity in protein-free fraction of plasma sample and C_p = amount of radioactivity in plasma sample.

DMD #12328

Results

Excretion of Radioactivity in Animals. Excreta from mice, rats, and monkeys were analyzed for radioactivity to assess the mass balance. Following oral administration, the mean recovery was high (Table 1, Figure 2). Fecal elimination was the primary excretory route observed in all species evaluated. Furthermore, bile-duct cannulated rats excreted the majority of the dose via the bile with low levels (7%) of the dose in the feces. Low levels of radioactivity were observed in the urine of rodents (up to 3.5%), whereas higher levels were recovered in monkey urine (18% of the dose). The excretory pathway was similar in monkeys given an IV bolus dose of [¹⁴C] naveglitazar (data not shown).

Pharmacokinetics of Naveglitazar, LY591026, and Radioactivity in Animals. The pharmacokinetic data for naveglitazar (*S*-enantiomer), LY591026 (*R*-enantiomer), and radioactivity are shown in Table 2. The plasma concentration versus time profiles are illustrated in Figure 3. [¹⁴C]naveglitazar was quickly absorbed and moderately metabolized prior to elimination. Following oral administration, 47, 31, and 62% of the radioactivity, as assessed by AUC values, were circulating as metabolites in mice, rats, and monkeys, respectively. LY591026 represented 8, 13, and 5% of the circulating metabolites in mice, rats, and monkeys, respectively or 3-4% of the total AUC. Half-lives for naveglitazar and radioactivity were similar within each species; however monkeys had substantially longer half-lives in comparison to mice and rats. Naveglitazar and radioactivity were slowly cleared from the system circulation in all species evaluated. The clearance of LY591026 appeared to be faster than the parent compound; however the calculated half-lives were likely underestimated due to the lack of quantifiable plasma concentrations of LY591026 in the terminal elimination phase.

In a separate study, rats received either a 10 mg/kg dose of naveglitazar (*S*-enantiomer) or LY591026 (*R*-enantiomer). The resulting pharmacokinetic parameters, which are shown in Table 3, indicate that both analytes are observed in the systemic circulation following the administration of either molecule.

DMD #12328

Plasma Protein Binding. The extent of *in vitro* binding of [³H]naveglitazar to plasma proteins was evaluated by ultracentrifugation in mouse, rat, and monkey plasma. The mean percentage \pm SEM of protein binding of radioactivity in plasma over the concentration range of 0.1 to 1000 ng/mL following *in vitro* incubation at 37°C for 60 minutes were 99.5% \pm 0.1% (mice), 99.6% \pm 0.1% (rat), and 99.6% \pm 0.3% (monkey). These results show that naveglitazar is highly bound to plasma proteins among the species examined and binding is independent of concentration.

In Vitro Metabolic Profiles from Liver Homogenates. The major metabolic pathway observed in human liver slices incubated in the presence of naveglitazar was the *para*-hydroxy metabolite (M2) with subsequent sulfate conjugation to M1 (Figure 4). In addition, dehydrogenation of the 2-methoxy propanoic acid chain was observed as a minor metabolic pathway, which led to the formation of M7. Small amounts of a sulfate conjugate of dehydrogenated naveglitazar + oxygen (M9) were also observed. The *in vitro* metabolic pathways observed in rat and monkey liver slices were similar to that in human liver slices. All metabolites observed in human liver slices were found in rat and monkey liver slices.

Metabolic Profiles of Excreta from Animals. Unchanged naveglitazar, the *para*-hydroxy metabolite (M2), and a dehydrogenated metabolite (M7) were observed in fecal extracts from all species evaluated (Table 4, Figure 5). M2 was the most prominent metabolite observed in fecal samples from mice, intact rats, and monkeys. M2 was isolated from fecal extracts and profiled using chiral chromatography to evaluate the presence of both enantiomers. Both enantiomers were observed across all species with the *R*-enantiomer, which is formed via chiral inversion, accounting for up to 40% of the total metabolite. These data suggest that when appropriate, both enantiomers of a metabolite may exist.

In bile cannulated rats, small amounts of M2 were observed in feces, however large amounts of the sulfate conjugate of the *para*-hydroxy metabolite (M1) were observed in bile (Table 4, Figure 5). In addition, glucuronide conjugates of naveglitazar (M13a-c), sulfate and glucuronide diconjugates of the *para*-hydroxy metabolite (M12a-c), and glucuronide conjugates of a dehydrogenated metabolite (M14a-b)

DMD #12328

were observed in rat bile. In mouse feces, naveglitazar, M1, M2, M7, dehydrogenated naveglitazar + oxygen (M8), a sulfate conjugate of dehydrogenated naveglitazar + oxygen (M9), and a taurine conjugate (M18) were observed. M1 and M2 were the most abundant metabolites observed.

No presence of naveglitazar was observed in monkey urine (Figure 6). Small amounts of M1, M2, a glucuronide conjugate of para-hydroxy naveglitazar (M3), and sulfate and glucuronide conjugates of hydroxylated diphenyl ether molecules (M15, M16, M17) were observed in monkey urine. None of these metabolites represented more than 3.5% of the recovered dose (Table 4).

Metabolic Profiles of Plasma in Animals. A total of six metabolites were observed in plasma across all species evaluated (Table 5). Naveglitazar represented the most abundant peak observed in circulation in all species (Figure 7). Small amounts of M1 and a phenyl acetic acid metabolite (M6) were also observed in all species. M2 was observed in monkey and mouse plasma.

Mass Spectrum of Naveglitazar and Major Metabolites (Figure 8). Full scan MS spectrum of parent drug showed the $[M+NH_4]^+$ ion at m/z 440. The product ion spectrum of m/z 440 gave the fragment ions at m/z 391 (loss of ammonia and methanol), m/z 377 (loss of ammonia and formic acid) and m/z 345 (loss of ammonia, methanol and formic acid). Loss of ammonia and 4-phenoxyphenol with subsequent loss of methanol or formic acid produced fragment ions at m/z 237, m/z 205, and m/z 191, respectively.

Comparison of the HPLC retention time and product ion mass spectrum with that obtained from the synthetic standard of naveglitazar confirmed the identification of parent peak.

M1 (sulfate conjugate of para-hydroxy naveglitazar). Full scan MS of M1 showed a $[M+NH_4]^+$ ion at m/z 536, corresponding to addition of an oxygen and a sulfate to parent drug. The product ion mass spectrum of m/z 536 produced the fragment ion at m/z 456 as the base peak (loss of 80 amu, suggesting the loss of a sulfate). MS^3 of m/z 536 \rightarrow m/z 456 produced fragment ions at m/z 439, m/z 407, m/z 361, m/z 205, and m/z 191, a similar fragmentation pattern as observed for para-hydroxy naveglitazar. After hydrolysis of plasma containing M1 with β -glucuronidase (with activity of sulfatase), the peak of M1 was

DMD #12328

converted to *para*-hydroxy naveglitazar. Comparison of the HPLC retention time and product ion mass spectrum with a synthetic standard of O-sulfate of *para*-hydroxy naveglitazar confirmed the identification of M1.

The NMR data for M1 also exhibited correlations very similar to naveglitazar. The absence of the H1 triplet and subsequent change of H2 to a doublet is consistent with the substitution of the O-sulphate group at position 1 (Table 6).

M2 (para-hydroxy naveglitazar). Full scan MS spectrum of M2 gave a $[M+NH_4]^+$ ion at m/z 456, corresponding to addition of an oxygen to parent drug. In the product ion mass spectrum of m/z 456, loss of ammonia and methanol with subsequent loss of formic acid produced the fragment ions at m/z 407 and m/z 361. The product ion at m/z 237 is corresponding to loss of 4-phenoxyphenol + O, suggesting that hydroxylation occurs on either of the aromatic rings of the di-phenyl ether moiety. Subsequent loss of methanol or formic acid from ion m/z 237 gave product ions at m/z 205 and m/z 191. Comparison of the HPLC retention time and characteristic product ions of M2 with that from a synthetic standard of *para*-hydroxy naveglitazar (LY621631) confirmed the identification of M2.

M6 (phenyl acetic acid metabolite). Full scan MS spectrum of M6 gave a $[M-H]^-$ ion at m/z 377. The product ion mass spectrum of m/z 377 produced the fragment ions at m/z 333 (loss of CO_2), m/z 185 (phenoxy phenol anion ion), m/z 151 (4-hydroxy phenyl acetic acid anion) and m/z 107 (loss of CO_2 from the 4-hydroxy phenyl acetic acid anion). Accurate mass measurement for M6 supports the proposed structure.

M7 (dehydrogenated naveglitazar). In positive ion mode, full scan MS spectrum of M7 gave a $[M+NH_4]^+$ ion at m/z 438, corresponding to parent $-H_2$. The product ion mass spectrum of m/z 438 gave fragments at m/z 421 (loss of ammonia) and m/z 403 (loss of ammonia and H_2O). In negative ion mode, full scan MS spectrum of M7 gave a $[M-H]^-$ ion at m/z 419. The product ion mass spectrum of m/z 419 produced the fragment ions at m/z 375 (loss of CO_2), m/z 343 (loss of CO_2 and methanol), m/z 185 (corresponding

DMD #12328

to the 4-phenoxyphenolated anion). The loss of 4-propoxyphenyl phenyl ether with subsequent loss of CO₂ gave the product ion at m/z 149. The existence of ion m/z 149 supports the assignment of the position of the dehydrogenation. The dehydrogenated naveglitazar standards (*trans*-, and *cis*-) were synthesized. Comparison of the HPLC retention time and product ion mass spectrum indicates that M7 has a *cis* conformation.

The NMR data for M7 exhibited correlations very similar to naveglitazar (Table 6). The aliphatic H19 and H20 resonances were not observed as in naveglitazar. H19 was instead observed as a singlet at 7.08ppm, indicative of the olefin bond. The long-range heteronuclear ³J_{H19-C21} coupling was observed to be 4.5Hz, indicative of a *cis* relationship between H19 and the acid moiety. (Breitmaier and Voelter, 1990).

M12a-c (sulfate and glucuronide diconjugate of M2). M12a-c was observed in bile from bile duct cannulated rats dosed with LY519818. Full scan MS of M12a-c gave a [M+NH₄]⁺ ion at m/z 712 and a [M-H]⁻ ion at m/z 693 in positive ion mode and negative ion mode, respectively, corresponding to addition of an oxygen, a sulfate and a glucuronic acid to parent drug. The product ion spectrum of m/z 712 gave a product ion at m/z 632 as a base peak (loss of sulfate). In the product ion spectrum of m/z 693, loss of sulfate or loss of glucuronide or loss of sulfate and glucuronide gave product ions at m/z 613 (base peak), m/z 517, and m/z 437, respectively. The product ion spectra for M12a to M12 c were similar, suggesting that they are isomers resulting from the acyl migration within glucuronic acid. After hydrolysis of rat bile with β-glucuronidase, all three peaks corresponding to M12a-c disappeared, and the peak of 4-hydroxy naveglitazar increased.

M13a-c (acyl glucuronide conjugate of naveglitazar). M13a-c in positive ion mode showed the [M+NH₄]⁺ ion at m/z at 616 (corresponding to additions of an ammonia and a glucuronic acid to naveglitazar) and in negative ion mode showed the [M-H]⁻ ion at m/z 597 (corresponding to addition of a glucuronic acid to naveglitazar). MS² of m/z 597 gave the aglycone ion at m/z 421 (base peak) and

DMD #12328

glucuronic acid anion at m/z 175. The MS^2 spectra for M13a-c were similar, suggesting that they are isomers resulting from the acyl migration within glucuronic acid.

M18 (taurine conjugate of naveglitazar). Full scan MS spectrum of M18 gave a $[M+NH_4]^+$ ion at m/z 547, indicating that the nitrogen content in M18 differs from that in the parent molecule. The product ion mass spectrum of m/z 547 produced the fragment ion at m/z 498 (loss of ammonia and methanol).

Subsequent loss of $NH_2CH_2CH_2SO_3H$ (125 amu) (characteristic fragmentation for a taurine conjugate) from the ion m/z 498 gave the fragment ion at m/z 373. Loss of 4-phenoxyphenol from the ion m/z 498 gave the fragment ion at m/z 312.

DMD #12328

Discussion:

Naveglitazar is a novel and potent PPAR α - γ dual, γ -dominant agonist that may be effective for the treatment of type 2 diabetes. These studies were conducted to characterize the disposition and metabolism of naveglitazar in mice, rats, and monkeys, which will aid in the safety assessment for this molecule as it relates to clinical practice. Additionally, *in vitro* liver slice incubations with naveglitazar were conducted to compare the metabolic pathways between animals and human. The metabolic pathways observed in rat and monkey liver slices were similar to that in human liver slices. Thus, all metabolites observed in human liver slices were found in rat and monkey liver slices.

Following administration of [^{14}C]naveglitazar, drug related material was well absorbed and slowly eliminated. Naveglitazar was the most abundant peak observed in circulation representing 76, 81, and 68% of the total radioactivity at T_{max} in the pooled plasma samples from mice, rats, and monkeys, respectively (Table 5). Since the metabolic profiling was conducted using reverse phase chromatographic techniques, these values represent the summation of naveglitazar and LY591026, which is formed *in vivo* from naveglitazar via chiral inversion. The mechanism for the chiral inversion is not clear; however it appears to be derived via an enzymatic process. Using rat liver homogenate, LY591026 could only be produced in the presence of the cofactors CoA and ATP. These data are similar to those reported for the enzymatic chiral inversion of ibuprofen, which was mediated by the formation of a thioester CoA intermediate followed by racemization (Knihinicki et al., 1989). In general, LY591026, which has a 10-fold less binding affinity for the PPAR γ receptor compared to naveglitazar, represents 3-4% of the total radioactive AUC in plasma, and 5-13% of the circulating metabolites observed across the animal species evaluated (Table 2). The metabolic chiral inversion is not unidirectional. In rats orally administered LY591026, exposure to both the naveglitazar (*S*-enantiomer) and LY591026 (*R*-enantiomer) was evident.

DMD #12328

LY621631 (M2), a phenyl acetic acid metabolite (M6), and/or the sulfate conjugate of M2 (M1) were detected in plasma from all three species. A few other small metabolites were also detected (Table 5). In general, LY591026 was the most abundant metabolite observed in plasma.

The primary route of excretion was the feces. In bile-duct cannulated rats, the majority of naveglitazar-related material was recovered in bile with only 7% of the dose recovered in the feces, indicating very good absorption of the material. The percent of recovered dose was similar across all species, ranging from 90-96% (Table 1), although the rate of excretion varied. In rodents, most of the naveglitazar-related material was recovered within a few days after dosing, whereas the rate of excretion in monkeys appeared to be slower (Figure 2). It is important to note that 4-14% of the dose was recovered in the carcass of rodents following the live-phase portion of the studies. The recovery in monkeys was slower than rodents during the first few days and a long noticeable elimination phase was observed following the first week of the recovery period. In general, approximately 10% of the dose was recovered during this period of time which is similar with the percent of dose recovered in rodent carcasses.

Since fecal elimination represented the major excretory pathway, it is important to evaluate the metabolic pathways observed in feces across the three species evaluated. Naveglitazar represented only 2 to 9% of the total dose administered, thus the majority of the radioactivity in feces was metabolites. Three major pathways were observed. In bile duct-cannulated rats, phase I oxidation and phase II conjugation resulted in three major metabolites, a sulfate and glucuronide diconjugate of *para*-hydroxy naveglitazar (M12a-c), a sulfate conjugate of *para*-hydroxy naveglitazar (M1), and an acyl glucuronide conjugate of naveglitazar (M13a-c). M1 and M12a-c likely result from the same pathway which accounted for 52.8% of the dose administered. Due to the functional groups located on separate ends of naveglitazar, it is not unexpected to observe a sulfate and glucuronide diconjugate. Following the consumption of red wine in humans, the abundant flavonoid catechin is metabolized to some degree to a sulfate and glucuronide diconjugate (Donovan et al., 1999). In addition, resorcinol is partial excreted in

DMD #12328

rats as a sulfate and glucuronide diconjugate (Kim and Matthews, 1987). M13a-c accounted for 14.2% of the dose. The *para*-hydroxy metabolite was not observed in bile, however this metabolite was observed in the feces of intact rats (48.9% of the dose) and monkeys (41.2% of the dose) where no phase II conjugation was detected. Thus, the conjugate forms were likely deconjugated once they entered the lower intestinal track via the bile duct. This pathway was also observed in the mouse, which represented 32.4% of the dose. An additional direct taurine conjugation of naveglitazar was observed in the mouse. This metabolite was only observed in feces and represented 11.1% of the dose. Six metabolites, none of which were higher than 3.5% of the dose, and no parent compound were detected in monkey urine (Figure 6).

In summary, the disposition and metabolism of LY519818 was characterized in mice, rats, and monkeys and the *in vitro* metabolic profile was assessed using liver slices from rat, monkey, and human. In general, the *in vitro* metabolic profile in human liver slices was similar to rat and monkey, although monkey displayed a slightly wider array of metabolites. In addition, the metabolic pathways observed *in vitro* were also observed *in vivo*. Following oral administration, naveglitazar was well absorbed and slowly eliminated. Studies in bile duct cannulated rats indicated that naveglitazar and associated metabolites were primarily eliminated via biliary excretion. The excretion profile was similar across all species evaluated, thus biliary excretion likely played a large role in mice and monkeys as well. Naveglitazar was metabolized by enzymatic chiral inversion, aromatic hydroxylation, oxidative dehydrogenation, and/or various phase II conjugation pathways (Figure 9). Although naveglitazar was moderately metabolized through both phase I and phase II metabolic processes, the primary circulating drug-related material was parent compound.

DMD #12328

Acknowledgments:

We want to express our appreciation to the animal studies personnel supporting Drug Disposition at Eli Lilly and Company for conducting the animal studies.

DMD #12328

References:

Auwerx J (1999) PPAR γ , the ultimate thrifty gene. *Diabetologia* **42**:1033-1049.

Bond M and Yates S (2004) Is the future bright for diabetes? *South Med J* **97**:1027-1028.

Breitmaier E and Voelter W (1990) *Carbon-13 NMR Spectroscopy*, 3rd Edition. VCH, New York.

Burke J, Williams K, Gaskill S (1999) Rapid rise in the incidence of type 2 diabetes from 1987 to 1996. *Arch Intern Med* **159**:1450-1460.

DeFronzo R (1992) Pathogenesis of type 2 (non-insulin-dependent) diabetes mellitus: A balanced overview. *Diabetologia* **35**:389-397.

Desvergne B, Michalik L, and Wahli W (2004) Be fit or be sick: Peroxisome proliferator-activated receptors are down the road. *Mol Endocrinol* **18**:1321-1332.

Diamant M and Heine R (2003) Thiazolidinediones in type 2 diabetes mellitus: Current clinical evidence. *Drugs* **63**:1373-1405.

Donovan J, Bell J, Kasim-Karakas S, German J, Walzem R, Hansen R, Waterhouse A (1999) Catechin is present as metabolites in human plasma after consumption of red wine. *J Nutr* **129**:1662-1668.

DMD #12328

Ferrannini E (1998) Insulin resistance versus insulin deficiency in non-insulin-dependent diabetes mellitus: Problems and prospects. *Endocr Res* **19**:477-490.

Keller H, Dreyer C, Medin J, Mahfoudi A, Ozato K, Wahli W (1993) Fatty acids and retinoids control lipid metabolism through activation of peroxisome proliferator-activated receptor-retinoid X receptor heterodimers. *Proc Natl Acad Sci USA* **90**:2160-2164.

Kersten S, Desvergne B, Wahli W (2000) Roles of PPARs in health and disease. *Nature* **405**:421-424.

Kim Y, Matthews H (1987) Comparative metabolism and excretion of resorcinol in male and female rats. *Fundam Appl Toxicol* **9**:409-414.

Knihinicki R, Williams K, Day R (1989) Chiral inversion of 2-arylpropionic acid non-steroidal anti-inflammatory drugs-1. *Biochem Pharmacol* **38**:4389-4395.

Liu Y and Reifel-Miller A (2005) Ligands to peroxisome proliferator activated receptors as therapeutic options for metabolic syndrome. *Drug Discovery Today: Therapeutic Strategies*. **2**:165-169.

Olefsky J (2000) Treatment of insulin resistance with peroxisome proliferator-activated receptor γ agonists. *J Clin Investig* **106**:467-472.

Prince M, Spicer K, Caro J, Abu-Raddad E, Konrad R, Wang M, Negrovilar A, and Danaberg J (2004) Efficacy of LY519818, a novel non-TZD, PPAR γ -dominant $\alpha\gamma$ dual agonist. *Diabetes* **52** (Suppl 2) A33.

DMD #12328

Rizvi A (2004) Type 2 diabetes: Epidemiologic trends, evolving pathogenic concepts, and recent changes in therapeutic approach. *South Med J* **97**:1079-1087.

Schoonjans K and Auwerx J (2000) Thiazolidinediones: An update. *Lancet* **355**:1008-1010.

Vandenbranden M, Wrighton S, Ekins S, Gillespie J, Binkley S, Ring B, Gadberry M, Mullins D, Strom S and Jensen C (1998) Alterations of the catalytic activities of drug-metabolizing enzymes in cultures of human liver slices. *Drug Metab Dispos* **26**:1063-1068.

DMD #12328

Footnotes:

Send reprint requests to Jason T. Johnson, Lilly Research Laboratories, Department of Drug Disposition,
Eli Lilly and Company, Lilly Corporate Center, Indianapolis, IN 46285, USA.

DMD #12328

Figures:

1. Structures of [¹⁴C]naveglitazar (*S*-enantiomer), LY591026 (*R*-enantiomer), and [¹³C]internal standard (compound 487748).
2. Recovery of naveglitazar-related material in the excreta following oral administration of [¹⁴C]naveglitazar in mice, rats, and monkeys. Symbols are: ●, mouse; ■, intact rat; □, bile-cannulated rat; and ▲, monkey.
3. Plasma concentration versus time profiles of naveglitazar, LY591026, and naveglitazar-derived radioactivity in mice, rats, and monkeys after administration of [¹⁴C]naveglitazar. Symbols are: ●, total ¹⁴C; ▲, naveglitazar; ■, LY591026.
4. HPLC-UV chromatograms of liver slice homogenates from rat, monkey, and human following in vitro incubations with naveglitazar.
5. HPLC radiochromatograms of feces from mice, rats, and monkeys and bile from rats following oral administration of [¹⁴C]naveglitazar.
6. HPLC radiochromatogram of monkey urine following oral administration of [¹⁴C]naveglitazar.
7. HPLC radiochromatogram of plasma from mice, rats, and monkeys following oral administration of [¹⁴C]naveglitazar.
8. Mass spectra for naveglitazar and major metabolites. naveglitazar; M2, *para*-hydroxy naveglitazar (LY621631); M1, sulfate conjugate of *para*-hydroxy naveglitazar; M12, sulfate and glucuronide diconjugate of *para*-hydroxy naveglitazar; M6, phenyl acid metabolite; M7, dehydrogenated naveglitazar; M18, taurine conjugate of naveglitazar.
9. Proposed major metabolic pathway for naveglitazar in mouse, rat, and monkey. M, mouse; R, rat; P, monkey.

DMD #12328

Table 1. Mean \pm SEM mass balance and route of excretion of naveglitazar-derived radioactivity in mice, rats, and monkeys following oral administration of [^{14}C]naveglitazar.

Species	Percentage of Dose Recovered				
	Urine	Feces	Bile	Carcass	Total ^a
Mouse (n=4)	3.5 \pm 0.1	82.6 \pm 2.3	NA	3.8 \pm 0.2	90.5 \pm 2.2
Rat (n=4)	1.0 \pm 0.0	74.6 \pm 1.3	NA	13.8 \pm 0.7	89.6 \pm 1.0
Cannulated Rat (n=4)	1.1 \pm 0.2	7.2 \pm 1.4	79.0 \pm 3.9	8.2 \pm 0.5	95.5 \pm 2.5
Monkey (n=4)	18.1 \pm 2.3	70.0 \pm 3.5	NA	NA	90.7 \pm 0.8

^a Percentage includes cage wash results.

NA= Not applicable.

DMD #12328

Table 2. Pharmacokinetics (Mean \pm SEM where appropriate) of naveglitazar (*S*-enantiomer), LY591026 (*R*-enantiomer), and radioactivity in mice, rats and monkeys following administration of [¹⁴C]naveglitazar.

	Mouse	Rat (n=3)	Monkey (n=4)	Monkey (n=4)
Dose/Route	10 mg/kg Oral	10 mg/kg Oral	5 mg/kg Oral	1 mg/kg IV
Naveglitazar				
C_{\max} ($\mu\text{g/mL}$)	16.4	49.3 \pm 2.43	44.0 \pm 3.3	23.9 \pm 525 ^a
$AUC_{0-\text{last}}$ ($\mu\text{g}\cdot\text{hr/mL}$)	97.0	254 \pm 7.75	499 \pm 35.2	94.0 \pm 9.43
$AUC_{0-\infty}$ ($\mu\text{g}\cdot\text{hr/mL}$)	97.3	254	515 \pm 45	94.0 \pm 9.43
T_{\max} (hr)	2.0	1.0	2.8 \pm 0.8	0 ^a
Half-life (hr)	53.8	14.3	199 \pm 75.3	32.3 \pm 4.3
CL/F (mL/min/kg)	1.71	0.66	0.16 \pm 0.02	0.18 \pm 0.02 ^b
V_{ss} /F (L/kg)	0.58	0.17	0.16 \pm 0.1	0.11 \pm 0.0 ^b
LY591026				
C_{\max} ($\mu\text{g/mL}$)	0.550	1.60 \pm 0.02	2.2 \pm 0.2	0.635 \pm 0.019
$AUC_{0-\text{last}}$ ($\mu\text{g}\cdot\text{hr/mL}$)	6.48	15.1 \pm 0.33	38.4 \pm 2.6	7.14 \pm 1.35
$AUC_{0-\infty}$ ($\mu\text{g}\cdot\text{hr/mL}$)	6.48	15.1	38.4 \pm 2.6	7.14 \pm 1.35
T_{\max} (hr)	4.0	2.0	3.5 \pm 0.5	1.5 \pm 0.3
Half-life (hr)	6.31	13.9	29.4 \pm 6.8	22.0 \pm 3.4
Radioactivity				

DMD #12328

C_{\max} ($\mu\text{g}\cdot\text{eq}/\text{mL}$)	21.2	59.2 ± 1.75	56.6 ± 2.5	21.8 ± 0.797^a
$\text{AUC}_{0-\text{last}}$ ($\mu\text{g}\cdot\text{eq}\cdot\text{hr}/\text{mL}$)	182	367 ± 9.75	1300 ± 150	224 ± 7.76
$\text{AUC}_{0-\infty}$ ($\mu\text{g}\cdot\text{eq}\cdot\text{hr}/\text{mL}$)	186	371	1300 ± 151	225 ± 7.76
T_{\max} (hr)	2.0	1.0	2.8 ± 0.8	0 ^a
Half-life (hr)	48.1	21.4	158 ± 16.9	166 ± 13.0
CL/F ($\text{mL}/\text{min}/\text{kg}$)	0.90	0.45	0.07 ± 0.01	0.07 ± 0^b
V_{ss}/F (L/kg)	0.80	0.21	0.20 ± 0.01	0.26 ± 0.03^b
% Naveglitazar of total radioactivity	53	69	38	42

^a Extrapolated values.

^b Represents true clearance and/or volume of distribution at steady state.

$\mu\text{g}\cdot\text{eq}$ = microgram equivalents of naveglitazar-related material.

DMD #12328

Table 3. Mean (n=4) pharmacokinetics of naveglitazar (*S*-enantiomer) and LY591026 (*R*-enantiomer) in rats following a 10 mg/kg administration of either naveglitazar or LY591026

Compound Administered	Naveglitazar		LY591026	
	Mean	SEM	Mean	SEM
Naveglitazar				
C_{\max} ($\mu\text{g/mL}$)	29.3	2.92	2.98	0.224
$AUC_{0-24 \text{ hr}}$ ($\mu\text{g}\cdot\text{hr/mL}$)	268	40.6	35.1	1.31
LY591026				
C_{\max} ($\mu\text{g/mL}$)	1.29	0.144	10.8	1.34
$AUC_{0-24 \text{ hr}}$ ($\mu\text{g}\cdot\text{hr/mL}$)	18.6	1.80	59.4	2.02

SEM=standard error.

Table 4. Estimated amount of naveglitazar and metabolites in excreta of mice, rats, and monkeys after oral administration of [¹⁴C]naveglitazar.

Compound	Mean % of dose ^a							
	Mouse	Intact Rat	Bile Cannulated Rat			Monkey		
	Feces	Feces	Feces	Bile	Total	Feces	Urine	Total
naveglitazar (includes LY591026)	5.2	9.0	3.2	3.1	6.3	1.7	ND	1.7
M1 (sulfate conjugate of <i>para</i> -hydroxy naveglitazar, LY2291229)	10.4	ND	ND	26.3	26.3	ND	2.9	2.9
M2 (<i>para</i> -hydroxy naveglitazar, LY621631)	22.0	48.9	0.7	ND	0.7	41.2	0.8	42.0
M3 (glucuronide conjugate of <i>para</i> -hydroxy naveglitazar)	ND	ND	ND	ND	ND	ND	0.8	0.8
M7 (dehydrogenated naveglitazar, LY2419535)	1.1	1.7	0.2	0.2	0.4	0.8	ND	0.8
M8 (dehydrogenated naveglitazar + O)	0.17	ND	ND	ND	ND	ND	ND	ND
M9 (dehydrogenated naveglitazar + O + sulfate)	0.04	ND	ND	ND	ND	ND	ND	ND
M12a-c (sulfate and glucuronide diconjugate of <i>para</i> -hydroxy naveglitazar)	ND	ND	ND	26.5	26.5	ND	ND	ND
M13a-c (acyl glucuronide conjugate of naveglitazar)	ND	ND	ND	14.2	14.2	ND	ND	ND
M14a-b (glucuronide conjugates of dehydrogenated naveglitazar)	ND	ND	ND	4.4	4.4	ND	ND	ND
M15 (glucuronide conjugate of 4,4'-dihydroxy diphenyl ether)	ND	ND	ND	ND	ND	ND	3.5	3.5
M16 (glucuronide conjugate of 4-hydroxy diphenyl ether)	ND	ND	ND	ND	ND	ND	0.2	0.2
M17 (sulfate conjugate of 4-hydroxy diphenyl ether)	ND	ND	ND	ND	ND	ND	0.7	0.7
M18 (taurine conjugate of naveglitazar)	11.1	ND	ND	ND	ND	ND	ND	ND
Total % of identified metabolites	50.0	59.6	4.0	74.6	78.7	43.6	9.6	53.2
Total % of radioactivity recovered in profiled excreta	72.3	72.6	5.6	76.4	82.0	57.9	11.7	69.6

^a The % of dose value was adjusted for feces by multiplying extraction recovery.

DMD #12328

Excreta used for quantitation were 0 to 24 hour feces for mice, 0 to 72 hour feces from intact rats, 0 to 48 hour bile and 0 to 24 hour feces from cannulated rats, 0 up to 168 hour feces and 0 to 48 hour urine from monkeys.

ND = not detected.

DMD #12328

Table 5. Estimated amount of naveglitazar and metabolites in pooled plasma from mice, rats, and monkeys after oral administration of [¹⁴C]naveglitazar.

Compound	% of plasma radioactivity ^a		
	Mouse ^b	Rat ^c	Monkey ^d
naveglitazar (includes compound 591026)	76.2	81.0	68.2
M1 (sulfate conjugate of <i>para</i> -hydroxy naveglitazar, LY2291229)	0.4	3.7	5.6
M2 (<i>para</i> -hydroxy naveglitazar, LY621631)	0.4	ND	7.5
M3 (glucuronide conjugate of <i>para</i> -hydroxy naveglitazar)	3.0	ND	ND
M6 (phenyl acetic acid metabolite)	3.8	NQ	NQ
M7 (dehydrogenated naveglitazar, LY2419535)	0.4	0.6	ND
M9 (dehydrogenated naveglitazar + O + sulfate)	NQ	ND	ND
M17 (sulfate conjugate of 4-hydroxy diphenyl ether)	0.6	ND	0.7
Total	84.8	85.3	82.0

^a The % of plasma radioactivity values were adjusted by multiplying extraction recoveries, which were 88%, 85%, and 82% for mouse, rat, and monkey plasma respectively.

Time points containing the highest level of radioactivity were used to pool samples to estimate analytes: ^b

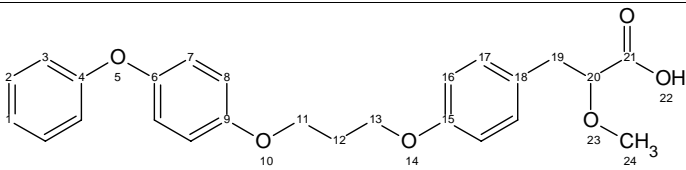
2 hour for mice, ^c 1 hour for rats, ^d 4 hour for monkeys.

ND = not detected.

NQ = detected but not quantifiable.

DMD #12328

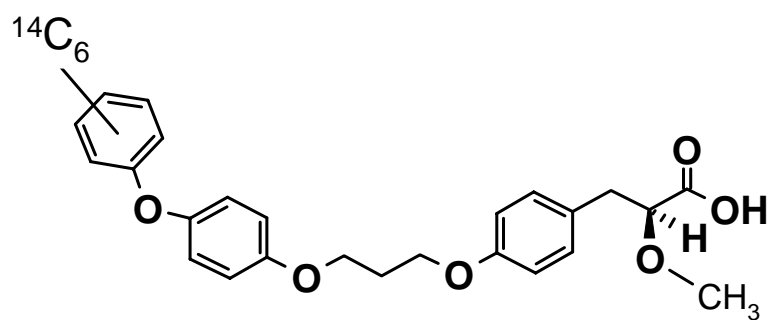
Table 6. NMR profile of naveglitazar, M1, and M7.



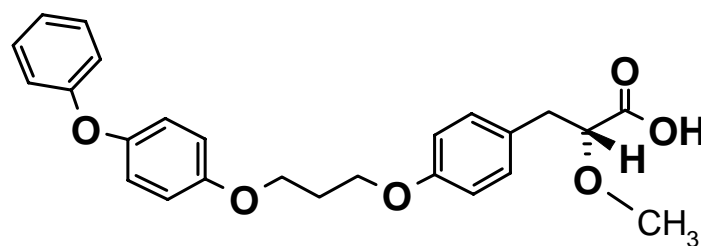
Position	$\delta^1\text{H}$ Multiplicity (<i>J</i> in Hz)			$\delta^{13}\text{C}$	
	Naveglitazar	M1	M7	Naveglitazar	M7
1	7.05 t (7.3)	--	7.03 t (7.4, 1.1)	122.4	122.5
2	7.30 dd (8.4, 7.3)	7.24 d (9.0)	7.29 dd (8.6, 7.4)	129.5	129.6
3	6.95 d (8.4)	6.97 d (9.0)	6.93 dd (8.6, 1.1)	117.5	117.7
4	--	--	--	158.5	158.5
6	--	--	--	150.2	150.5
7	6.98 d (9.0)	7.00 AB	6.96 d (9.1)	120.8	120.9
8	6.90 d (9.0)	7.00 AB	6.89 d (9.1)	115.5	115.3
9	--	--	--	155.2	155.1
11	4.15 t (6.0)	4.20 t (6.3)	4.14 t (6.0)	64.6	64.8
12	2.26 p (6.0)	2.20 p (6.3)	2.27 p (6.1)	29.4	29.4
13	4.16 t (6.0)	4.20 t (6.3)	4.18 t (6.1)	64.6	64.5
15	--	--	--	157.9	159.7
16	6.86 d (8.6)	6.92 d (8.6)	6.91 d (8.4)	114.5	115.0
17	7.16 d (8.6)	7.17 d (8.6) s	7.70 d (8.5)	130.4	132.1
18	--	--	--	128.3	132.0
19	2.98 dd (14.4, 7.3)	2.91 dd (14.2, 5.2)	7.08 s	37.4	125.5
	3.10 dd (14.4, 4.2)	3.02 dd (14.2, 7.0)			
20	4.00 t (7.3, 4.3)	4.10 br	--	81.3	144.1
21	--	--	--	174.1	169.3
24	3.41 s	3.30 s	3.75 s	58.7	59.2

s = singlet, d = doublet, t = triplet, p = pentet, br = broad, dd = doublet of doublets, AB = center of AB doublets.

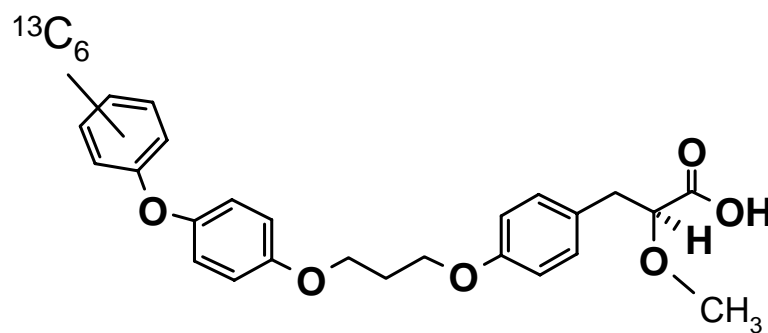
Figure 1



[^{14}C]Naveglitazar



LY591026



[^{13}C]Internal Standard

Figure 2

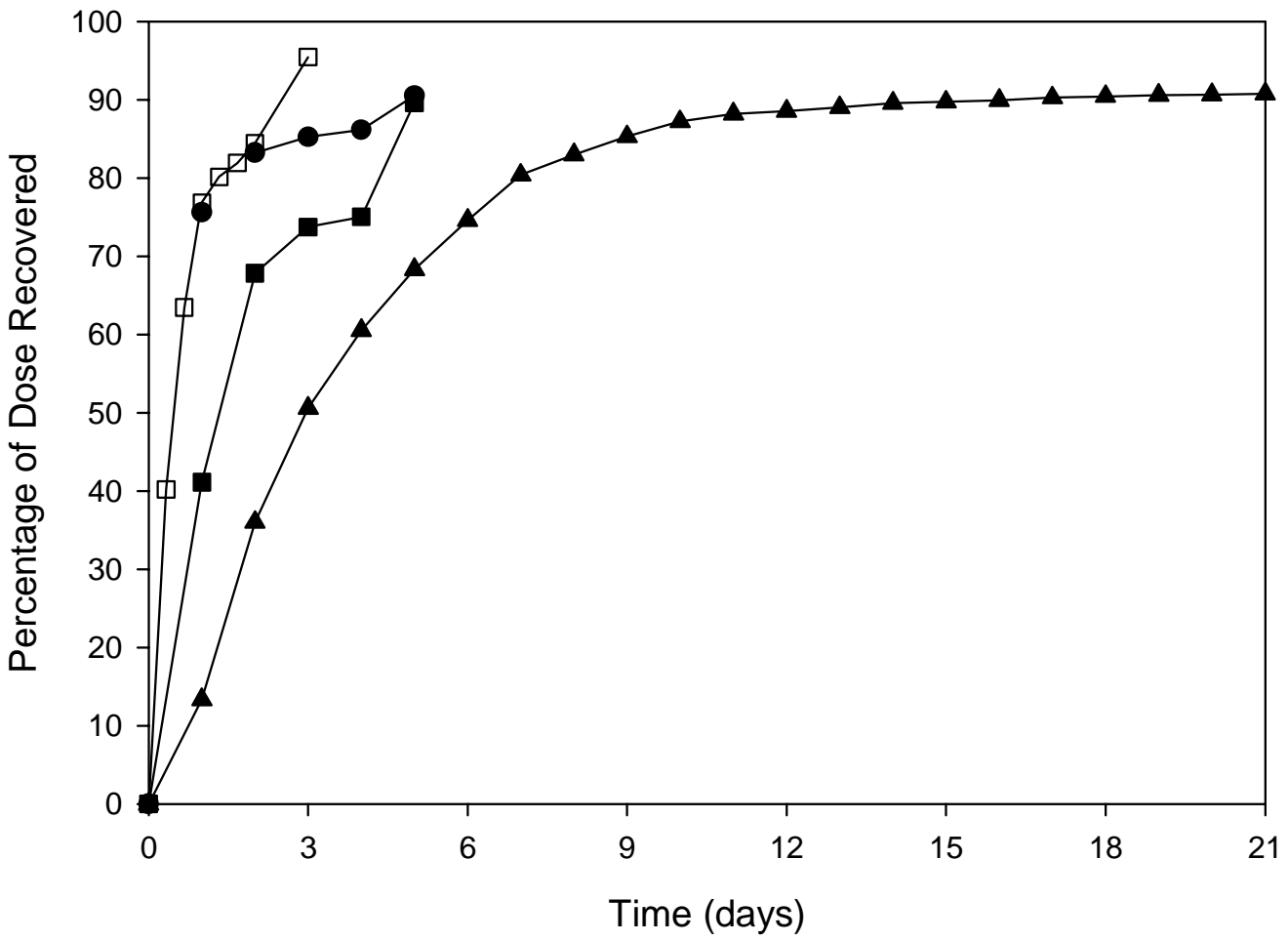


Figure 3

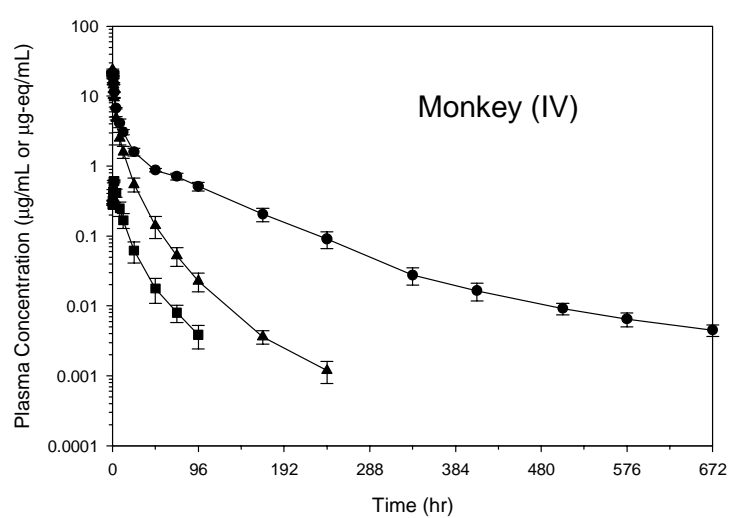
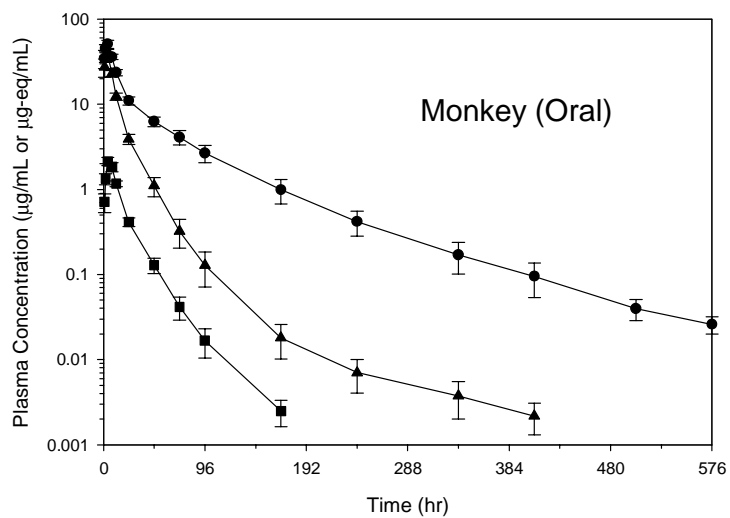
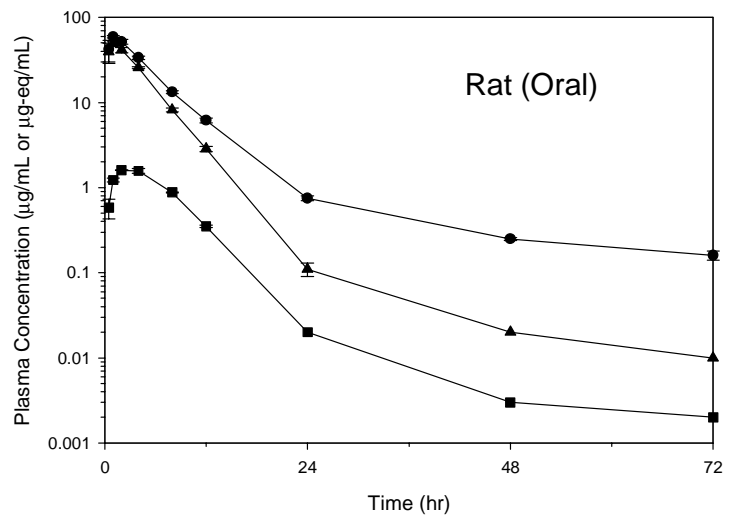
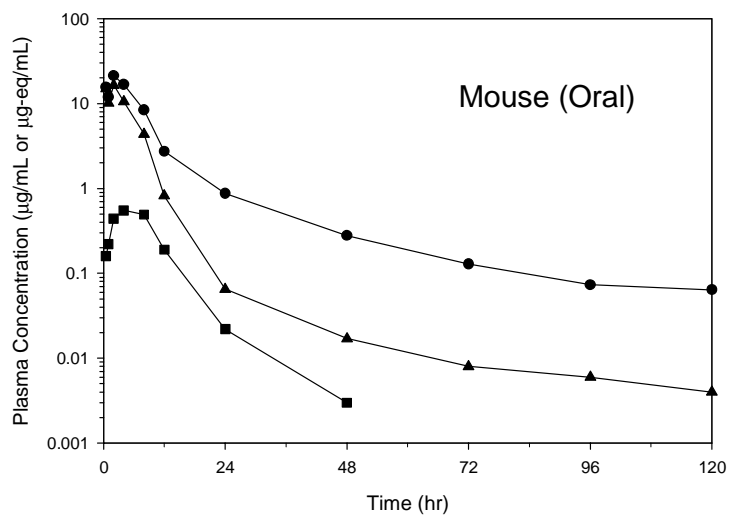


Figure 4

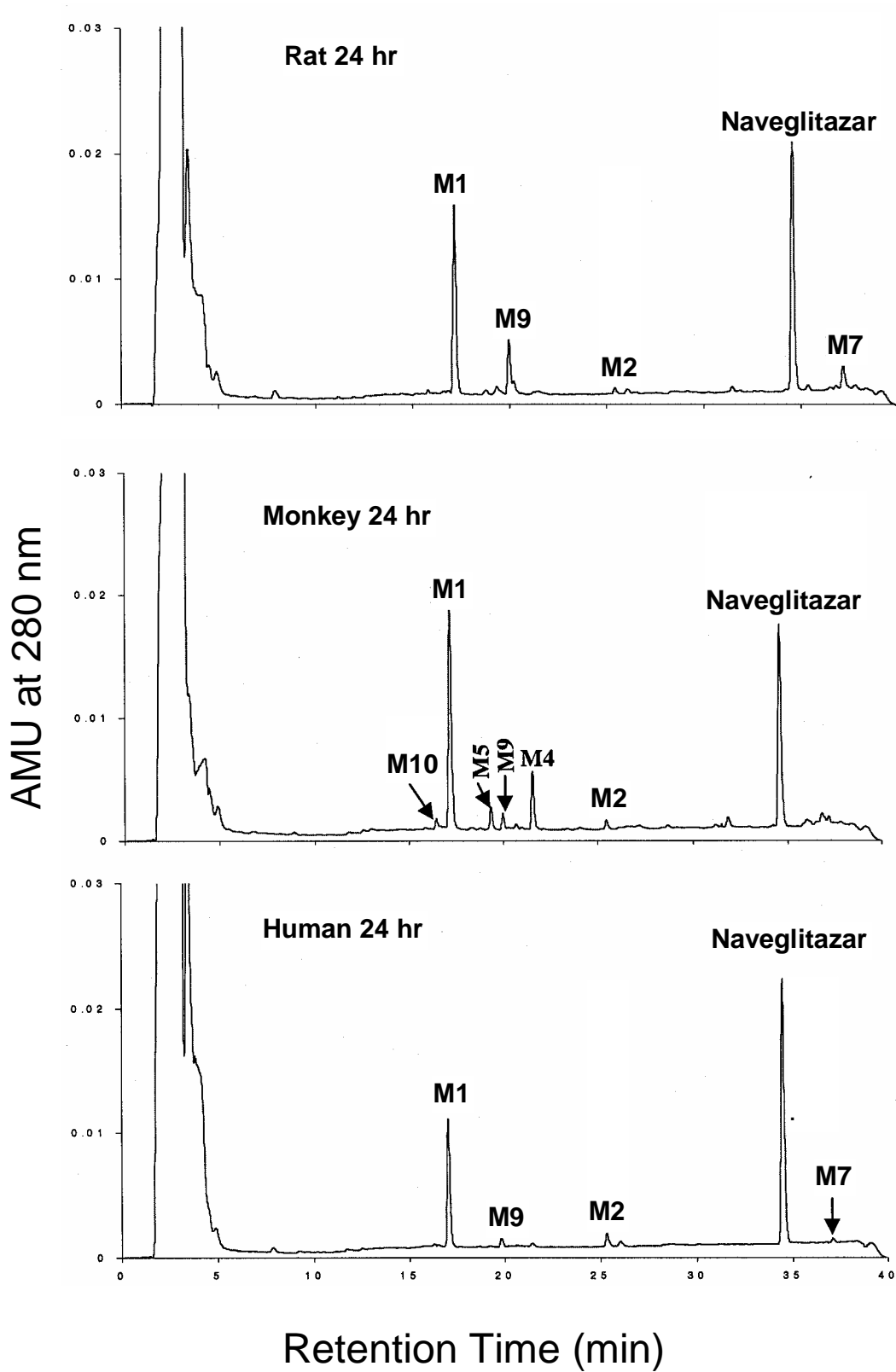


Figure 5

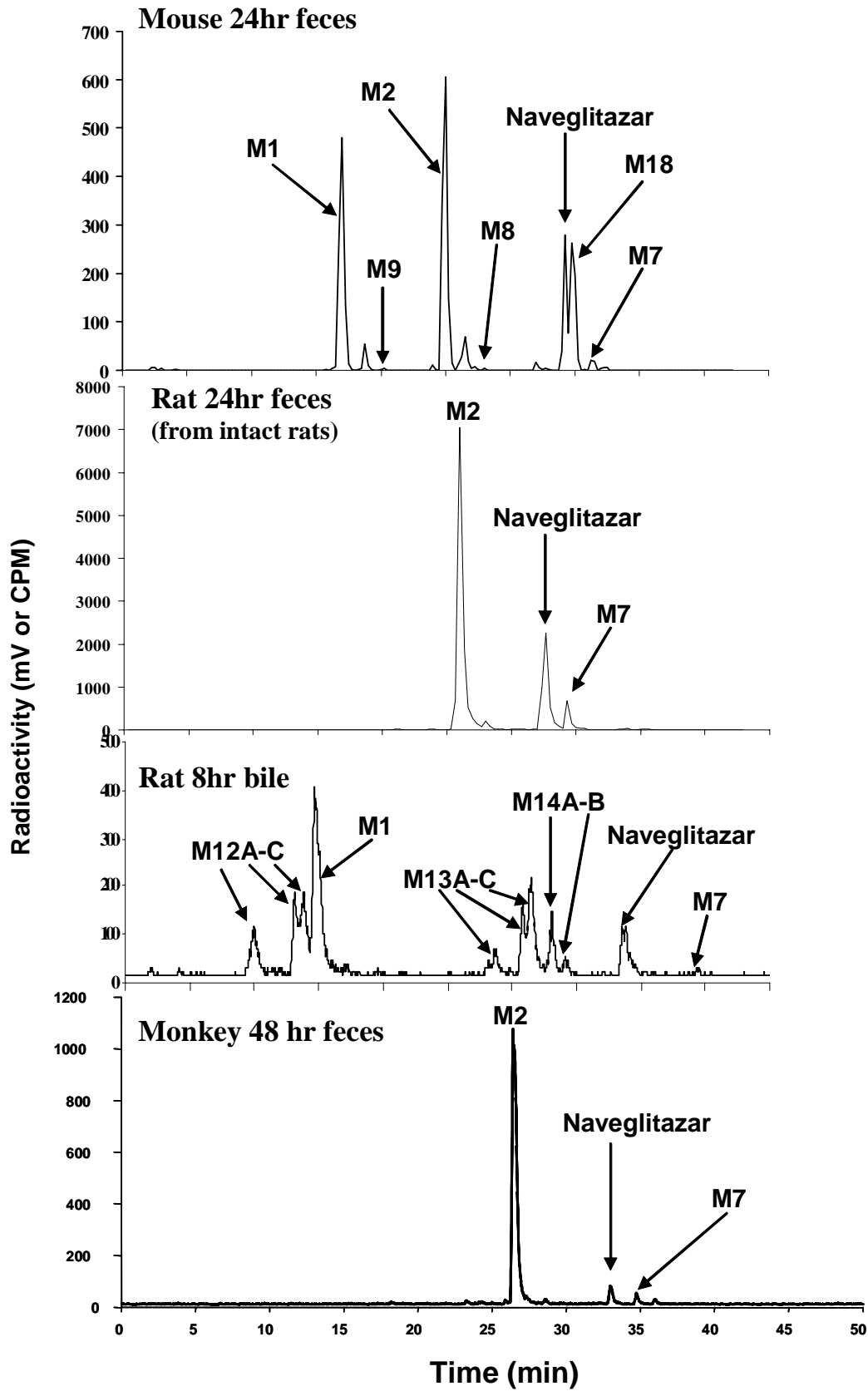


Figure 6

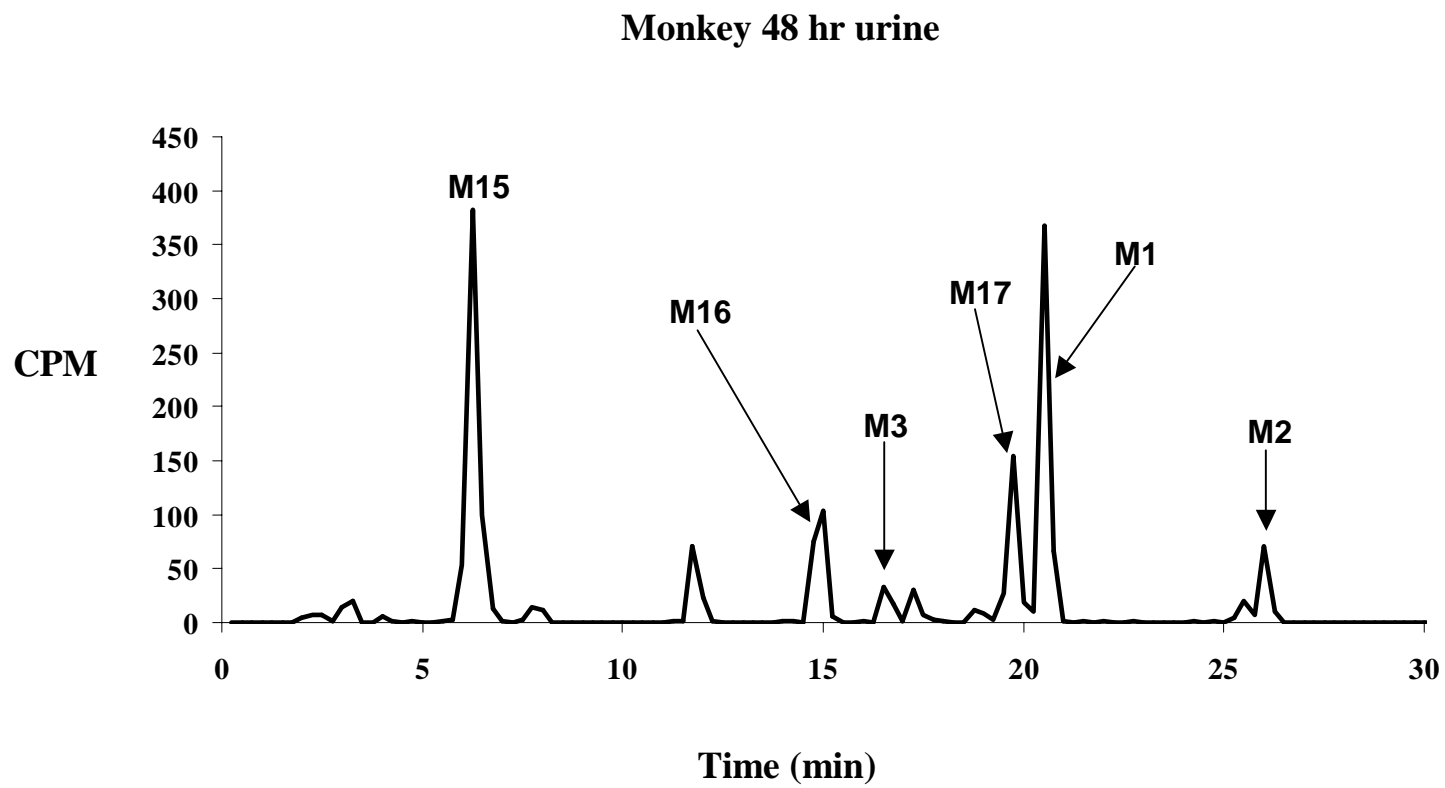


Figure 7

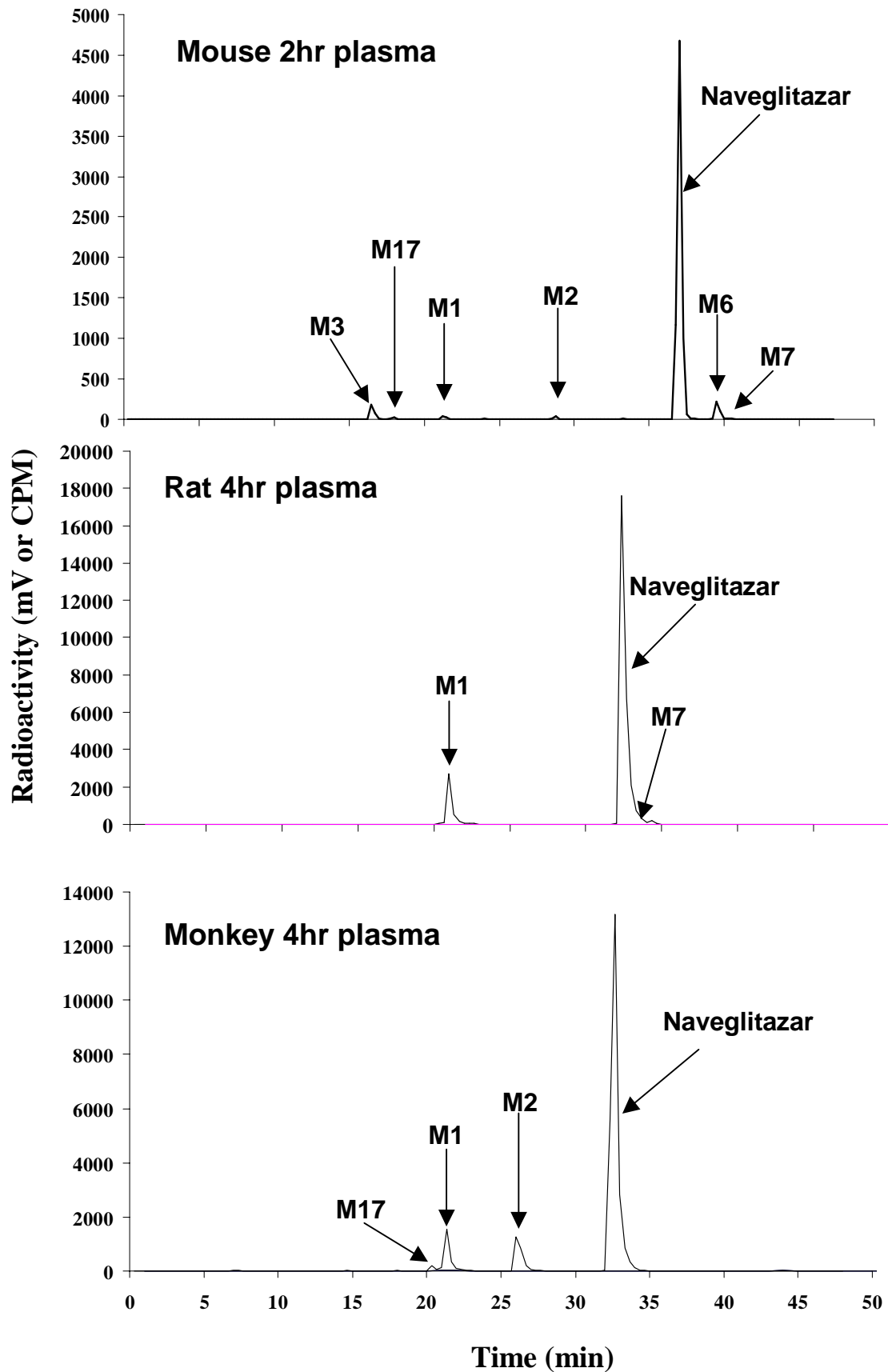


Figure 8

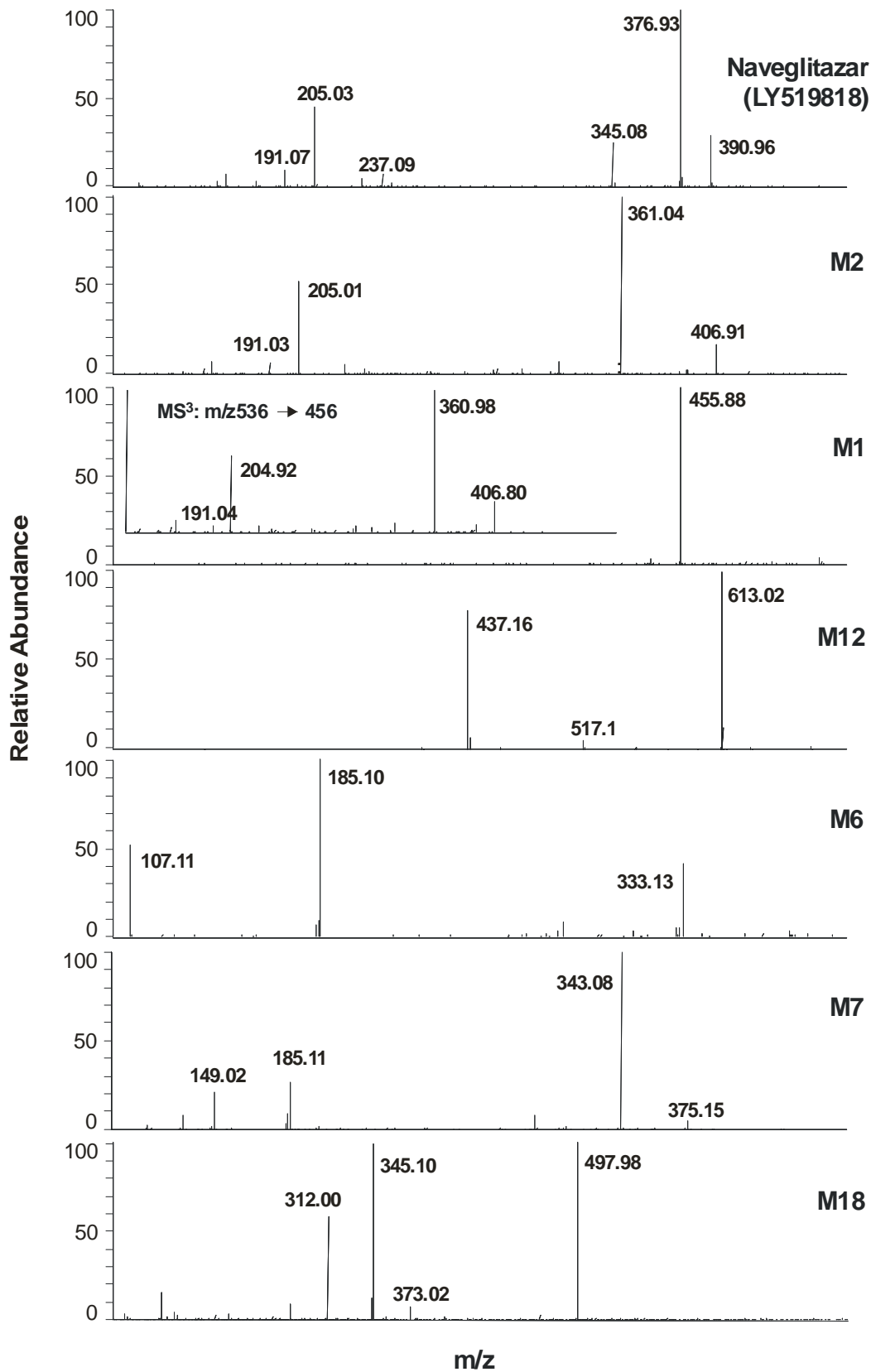


Figure 9

